Surface Science 604 (2010) 692–700

Contents lists available at ScienceDirect

Surface Science

journal homepage: www.elsevier.com/locate/susc

Investigation of the structural and dynamical properties of the (0 0 1) surface of $LiCu_2O_2$

Yangyang Yao [a], Xuetao Zhu [a], H.C. Hsu [b], F.C. Chou [b], M. El-Batanouny [a,*]

[a] Physics Department, Boston University, Boston, MA 02215, United States
[b] Center of Condensed Matter Sciences, National Taiwan University, Taipei 10617, Taiwan

ARTICLE INFO

Article history:
Received 19 October 2009
Accepted for publication 22 January 2010
Available online 4 February 2010

Keywords:
$LiCu_2O_2$
Helium atom scattering
Surface structure
Surface dynamics
Surface phonons

ABSTRACT

We report on studies of the structure and dynamics of the (0 0 1) surface of single crystal $LiCu_2O_2$, investigated by He beam scattering at room temperature, and with lattice-dynamical models. The best fit surface corrugation to measured diffraction patterns shows that the surface termination is exclusively a $Li^{1+}Cu^{2+}O^{2-}$ plane. Lattice dynamics fits to inelastic He scattering spectra reveal the presence of two low-lying surface phonon modes, identified with the motion of Cu^{2+}, Li^{1+} surface ions normal to the surface.

1. Introduction

$LiCu_2O_2$ continues to attract considerable attention because of the unique physical properties it exhibits. Initially, interest in this system was stimulated by the presence of double-chain ladders of $Cu^{2+}O$, which presented a prototypical quasi-one-dimensional (Q1D) spin-1/2 quantum magnetic system with competing magnetic interactions. Such competing interactions in the classical double-chain ladder were known to give rise to geometric frustration, which in turn is manifest in an ordered incommensurate helimagnetic phase at low temperatures. It was expected that the presence of $S = 1/2$ spins would give rise to strong commensurate quantum spin fluctuations that tend to suppress magnetic order [1–5]. More recently, it was discovered that this system exhibits ferroelectricity upon the emergence of helicoidal magnetic order. This renders $LiCu_2O_2$ as the second cuprate to join the list of multiferroics [6–9].

Electron spin resonance (ESR) measurements revealed the presence of a dimerized spin-singlet ground state at $T > T_N = 24.6$ K, with an energy gap of $\Delta = 72$ K between this state and the first spin-triplet excited state [10]. Below T_N a collinear sinusoidal spin-ordered phase with polarization along the *c*-axis and a modulation wave vector of $\mathbf{Q} = (0, 0.172, 0)$ r.l.u. was reported [11,12]. A second magnetic phase transition was reported to occur at $T_{FE} \simeq 23.0$ K. Below this temperature, an ordered helicoidal magnetic phase appears, where the spin polarization acquires small components along the *a* and *b* axes [1,11,13,12]. The onset of the helicoidal phase induces ferroelectricity with polarization along the *c*-axis [6,9].

$LiCu_2O_2$ is a quasi-1D insulator. It has a layered charge-ordered orthorhombic crystal structure belonging to the *Pnma* space group; the primitive cell has lattice constants $a = 5.73$ Å, $b = 2.86$ Å, $c = 12.47$ Å respectively [14]. It is a mixed-valent compound with copper ions in the Cu^{2+} and Cu^{1+} valence states. The magnetic Cu^{2+} ($S = 1/2$) ions are located at the center of edge-sharing CuO_4 plaquettes which form infinite chains along the crystallographic *b*-axis. Coplanar chains are connected by chains of Li ions along the *a*-axis, and two such planes form double-layers parallel to the *ab*-plane, as shown in Fig. 1. The Q1D spin arrangement is due to these double-chains of Cu^{2+} ions that run along the crystallographic *b* axis. The period of each leg of the double spin chains is equal to *b*. The two legs are offset by b/2 relative to each other. Along the *c*-axis, each double-layer is separated from its double-layer neighbors by magnetically inert Cu^{1+} planes.

Despite the extensive studies of bulk structural and magnetic properties of $LiCu_2O_2$ crystals cited above, no investigation of its surface properties has been reported in the literature. It is known that $LiCu_2O_2$ crystals easily peel along the (0 0 1) surface. However, since these crystals consist of alternating double-layers of $Li^{1+}Cu^{2+}O_2^{2-}$ and single layers of Cu^{1+}, it remains to be determined whether the cleavage would result in the coexistence of $Li^{1+}Cu^{2+}O_2^{2-}$ and Cu^{1+} surfaces, or in an exclusive presence of one of these layer types. If the latter scenario occurs, then it would dictate that the double-layer must split in order to provide complete coverage of the two newly exposed surfaces. The double-layer

---

* Corresponding author.
E-mail address: elbat@bu.edu (M. El-Batanouny).

0039-6028/$ - see front matter © 2010 Elsevier B.V. All rights reserved.
doi:10.1016/j.susc.2010.01.017

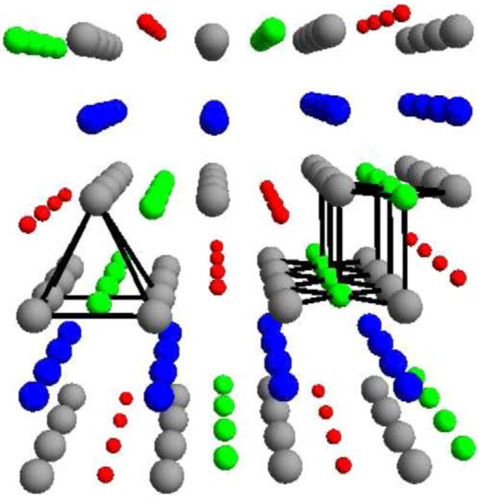

Fig. 1. Crystal structure of $LiCu_2O_2$. The color code is: Li (red), O (gray), Cu^{1+} (blue), Cu^{2+} (green). (For interpretation of the references to colour in this figure legend, the reader is referred to the web version of this article.)

splitting means the splitting of the double-chain and the presence of a single-chain, which is expected to display different magnetic behavior from that observed in the double-chain.

In this paper we present the results of extensive studies of the (001) surface of $LiCu_2O_2$, using the experimental techniques of elastic and inelastic helium scattering aimed at determining its surface structural and dynamical properties, respectively. Furthermore, we used lattice-dynamical models with slab geometries to interpret the surface phonon dispersion curves derived from the measured inelastic scattering spectra. As we will demonstrate below, the surface corrugation topography, derived from a large set of measured diffraction patterns, clearly shows that the surface termination is exclusively $Li^{1+}Cu^{2+}O_2^{2-}$. Moreover, empirical lattice dynamics models, with slab geometries based on such termination and fit to the inelastic experimental results, reveal two low-lying dispersion curves with polarizations normal to the surface, one involves Cu^{2+} and the second involves Li^{1+} ions. In Section 2 the experimental setup and procedures are discussed, and the results and conclusion are presented in Section 3.

2. Experimental setup and procedure

Single crystals of $LiCu_2O_2$ with high Li content of $\simeq 0.99 \pm 0.03$ were grown by the floating-zone method. The Li content was determined accurately through combined iodometric titration and thermogravimetric methods. This ruled out the possibility of chemical disorder between Li and Cu ions. Details of the growth procedures and stoichiometry confirmation are given in Ref. [15]. Typical crystal samples used were about 3 mm × 3 mm × 2 mm in size, with its exposed surface parallel to the *ab*-plane. The crystals were attached to an OFHC copper sample-holder by conductive silver epoxy. A cleaving (peeling) post was attached to the top sample surface in a similar way. The prepared sample-holder was mounted on a sample manipulator equipped with *XYZ* motions as well as polar and azimuthal rotations. The pressure in the Ultra-High Vacuum (UHV) chamber was maintained at 10^{-10} torr throughout the experiment to ensure cleanliness of the sample surface during measurement performance. In situ cleaving under UHV conditions was effected by knocking off the cleaving post. Immediately after cleaving, the quality of the long-range ordering on the surface was confirmed by the appearance of sharp diffraction LEED spots.

A supersonic mono-energetic collimated helium beam, with velocity resolution better than 1.4%, was generated by a nozzle-skimmer assembly and 2mm diameter collimating slits. The average beam velocity was varied by attaching the nozzle reservoir to a closed-cycle helium refrigerator, and controlling the reservoir temperature with the aid of a digital temperature controller (Scientific Instruments Model 9700) and a diode sensor attached to the reservoir. As a result, the beam energy can be varied in the range 65–21 meV by varying the nozzle temperature from 300 K to 110 K, respectively. Polar rotation of the sample was used to vary the incident angle θ_i with respect to the surface normal, while the azimuthal rotation was employed to align the scattering plane along a high-symmetry surface crystallographic direction. The scattered He beam was collected by an angle-resolved detector mounted on a two-axis goniometer, which allows the scattered angle θ_f to be varied independently from θ_i [16], and allows in- and out-of the scattering-plane measurements. The detector [17] is comprised of an electron gun and a multichannel plate (MCP) electron multiplier. The electron gun generates a well-collimated, mono-energetic electron beam crossing the He beam at right angles. The energy of the electron beam is tuned to excite the He atoms to their first excited metastable state (2^3S He^*) upon impact. Deexcitation of a He^* atom at the surface of the MCP leads to the ejection of an electron which generates an electron cascade that is then collected by the anode of the multiplier. By electronically pulsing the electron gun, a gate function is created for time-of-flight (TOF) measurements in the inelastic HAS mode. The details of the detection scheme are given in Ref. [17]. All measurements were performed with the sample surface at room temperature.

By writing the He-atom wave vector as $\mathbf{k} = (\mathbf{K}, k_z)$, where $\mathbf{K}$ is the component parallel to the surface, conservation of momentum and energy for in-the-scattering-plane geometry can be expressed as

$$\Delta\mathbf{K} = \mathbf{G} + \mathbf{Q} = k_f \sin\theta_f - k_i \sin\theta_i, \tag{1}$$

$$\Delta E = \hbar\omega(\mathbf{Q}) = E_f - E_i = \frac{\hbar^2}{2M}(k_f^2 - k_i^2), \tag{2}$$

where subscripts i and f denote incident and scattered beams, respectively, and $\Delta\mathbf{K}$ is the momentum transfer parallel to the surface. $\mathbf{G}$ is a surface reciprocal-lattice vector, $\mathbf{Q}$ is the surface phonon wave vector, and $\hbar\omega(\mathbf{Q})$ is the corresponding surface phonon energy. $E_{i,f} = \hbar^2 k_{i,f}^2/2M$, where M is the mass of a He atom. By eliminating $\mathbf{k_f}$ from the above equations, one obtains the so-called scan curve relations which are the locus of all the allowed $\Delta\mathbf{K}$ and ΔE as dictated by the conservation relations,

$$\Delta E = E_i\left[\left(\frac{\sin\theta_i + \Delta\mathbf{K}/k_i}{\sin\theta_f}\right)^2 - 1\right]. \tag{3}$$

The intersections of these scan curves with the phonon dispersion curves define the kinematically allowed inelastic events for a fixed geometric arrangement. Thus, by systematically changing E_i, θ_i, and θ_f, the entire dispersion curves can be constructed.

3. Results and discussion

3.1. Elastic he scattering and surface structure

Diffraction patterns were collected from many crystal samples at a temperature of 300 K for several scattering conditions:

(1) incident He wave numbers, k_i, in the range 6.42 $Å^{-1}$ and 11.12 $Å^{-1}$,
(2) incident angles, θ_i, between 30° and 50°, and
(3) two high-symmetry azimuthal surface orientations, *a* and *b*, separated by 90°.

As was mentioned above, there are two candidates for the surface termination, which are shown in Fig. 2, the $Li^{+1}Cu^{2+}O_2^{2-}$ layer and the Cu^{1+} layer. The former has a rectangular lattice, while the